Proceedings of the 11th Brazilian Congress of Thermal Sciences and Engineering – ENCIT 2006
Braz. Soc. of Mechanical Sciences and Engineering – ABCM, Curitiba, Brazil, Dec. 5-8, 2006

Paper CIT06-0851

STABILITY OF THE CHEMICAL AND HYDRODYNAMIC FIELDS CLOSE TO A ROTATING DISK ELECTRODE: NON-SYNCHRONOUS PERTURBATIONS

J. Pontes
Metallurgy and Materials Engineering Department/EP-COPPE – Federal University of Rio de Janeiro
PO Box 68505 21941-972 Rio de Janeiro RJ, Brazil
`jopontes@metalmat.ufrj.br`

N. Mangiavacchi
Mechanical Engineering Department, State University of Rio de Janeiro
R. São Francisco Xavier 524 20550-013 Rio de Janeiro, RJ, Brazil
`norberto.mangiavacchi@gmail.com`

O. E. Barcia
Institute of Chemistry/IQ – Federal University of Rio de Janeiro
PO Box 68505 21941-972 Rio de Janeiro RJ, Brazil
`barcia@metalmat.ufrj.br`

O. R. Mattos
Metallurgy and Materials Engineering Department/EP-COPPE – Federal University of Rio de Janeiro
PO Box 68505 21941-972 Rio de Janeiro RJ, Brazil
`omattos@metalmat.ufrj.br`

B. Tribollet
UPR15 – CNRS, Physique des Liquides et Electrochimie
4 place Jussieu, 75252 Paris Cedex 05, France
`bt@ccr.jussieu.fr`

Abstract. *Polarization curves experimentally obtained in the electro-dissolution of iron in a* 1 M $\mathbf{H_2SO_4}$ *solution using a rotating disk as the working electrode present a current instability region within the range of applied voltage in which the current is controlled by mass transport in the electrolyte. According to the literature (Barcia, 1992) the electro-dissolution process leads to the existence of an axial viscosity gradient in the interface metal-solution, which leads to a deviation from von Kármán's classical solution for rotating disk flow. On two previous papers, Pontes et al (J. of the Braz. Soc. Mechanical Sciences, Vol. XXIV, pp. 139, 2002, and Phys. of Fluids, Vol. 16, No. 3, pp. 707, 2004) showed that stability of the steady flow, affected by a time-independent viscosity gradient pointing in the axial directions, is strongly affected by the stratified viscosity profile. In this work, we go one step beyond, by considering the stability of the hydrodynamic field, coupled through the viscosity, to the chemical field originated by the transport of one species. A phenomenological law is assumed, relating the viscosity to the concentration of chemical species. The viscosity at the interface with the electrode is estimated by relating the experimental value of the current density, to the concentration gradient of the relevant chemical specie at that point. The steady state of the problem is obtained and a linear stability analysis of the coupled fields is made. The resulting eigenvalue-eigenfuction problem is presented, as well as the neutral stability curves for disturbances turning with the same angular velocity of the disk (stationary) and for disturbances turning with angular velocity different from the disk one(non-stationary).*

keywords: *Rotating Disk, Hydrodynamic Stability, Electrochemistry*

1. Introduction

Electrochemical cells using a rotating disk electrode are a widely used experimental tool in electrochemistry, due the simplicity of the setup and the fact that the mass flux is independent of the radial position along the disk, at steady state conditions (Levich, 1962). Furthermore, the rate of transfer of ions close of the electrode is conveniently controlled by imposing an adequate angular velocity to the electrode. This rate of transfer defines the maximum steady state current attained in an experiment.

Two current instabilities are observed in the region where the current is controlled by mass transport (Ferreira *et al.*, 1994). The first instability is intrinsic to the system, while the current instability close to the active-passive transition is affected by the output impedance of the control equipment. This instability can be suppressed by using a negative feedback resistance (Epelboin *et al.*, 1979), that gives rise to a continuous transition.

Most explanations presented in the literature for the current instabilities are based on mechanisms proposing a $\mathbf{FeSO_4}$ film precipitated at the electrode surface (Russel and Newman, 1986). In fact, changes in the ohmic voltage drop due to precipitation and dissolution of a $\mathbf{FeSO_4}$ film provide an acceptable explanation for the instability observed in the active/passive transition region, coupled with the output impedance of the control equipment. However, this model can not be generalized to explain oscillations observed at the beginning of the current plateau. Indeed, using electro-hydrodynamic (EHD) impedance measurements (Tribollet and Newman, 1983), Barcia *et al.* (1992) studied the electro-dissolution of iron electrodes in 1 $\mathbf{M}$ $\mathbf{H_2SO_4}$ at the current plateau, before and after the first instability region. They propose that the electro-dissolution process leads to the existence of a viscosity gradient in the diffusion boundary layer, which could affect the stability of the hydrodynamic field and explain the observed current instability.

To investigate the importance of the hydrodynamics in the electro-dissolution of iron, Ferreira *et al.* (1994) and Geraldo *et al.* (1998) studied the influence of the viscosity on the current oscillations observed at the beginning of the current plateau region of the above described experiment. These authors found that increasing the bulk electrolyte viscosity – and therefore decreasing the Reynolds number of the experiment – by adding glycerol to the solution, the current signals evolve from chaotic to periodic, and to a stationary regime, where the instability is suppressed. They also found that the current oscillations are enhanced by an increase in the angular velocity of the electrode.

The existence of a hydrodynamic instability in rotating disk flow has been the object of a number of investigations, both experimental and theoretical in the case of fluids with uniform viscosity. The main result shows that the steady flow becomes unstable beyond a certain non-dimensional distance from the axis of rotation.

The flow develops corotating vortices which spiral outward with their axes along logarithmic spirals of angle $90^\circ + \varepsilon$ ($\varepsilon \approx 13^\circ$) with respect to radius of the disk. Malik (1986) determined the neutral stability curve for stationary vortex disturbances, which turn with the angular velocity of the disk. Neutral curves were presented in the $\alpha \times R$, $\beta \times R$ and $\varepsilon \times R$ planes for zero-frequency disturbances, where α and β are the components of the real perturbation wave-vector along the radial and azimuthal directions and ε is the angle between the perturbation and the radial direction, given by $\varepsilon = \tan^{-1} \beta/\alpha$. The critical Reynolds number was found to be in good agreement with experimental results, at a value of $R = 285.36$.

A comprehensive review of the literature on the subject, concerning research made until 1989 can be found in the paper by Reed and Saric (1989).

Faller (1991) determined the neutral stability curves for setup configurations consisting of rotating or stationary disks and flows approaching the disk with (rotating flow) or without (stationary flow) bulk angular velocity. Critical Reynolds number for the case of rotating disk and stationary fluid was found as 69.4.

Lingwood (1995) presented the neutral curve for vortices turning with several angular velocities and theoretical results concerning the asymptotic response of the flow to an impulsive excitation exerted in the flow at a certain radius at $t = 0$. Additionally, Lingwood's work addresses the case where the wavenumber component along the radial direction, α, is complex, leading to an exponential growth along that direction. The curve for this case defines the region of absolute instability, with a critical Reynolds number of $R = 510.625$.

It is well known that boundary layers can be destabilized by increasing the viscosity close to the wall and stabilized by decreasing, through heating or cooling the wall (Schlichting and Gersten, 1999). Schäfer *et al.* (Schäfer *et al.*, 1995) deduced an asymptotic expression for the critical Reynolds number for moderate temperature differences in boundary layers developed over flat plates, taking into account the temperature dependency of the viscosity. Turkyilmazoglu Cole and Gajjar (1998)) studied the influence of heat transfer on the convective and absolute instability of compressible boundary layers in rotating disk flow.

On two previous papers, Pontes *et al.* (2002, 2004) , showed that stability of the steady flow, affected by a time-independent viscosity gradient pointing in the axial directions, is strongly affected by the stratified viscosity profile. In this work, we go one step beyond, by considering the stability of the hydrodynamic field, coupled through the viscosity, to the chemical field resulting from the transport of the relevant chemical specie. A phenomenological law is assumed, relating the viscosity to the concentration of chemical specie. The viscosity at the interface with the electrode is estimated by relating the experimental value of the current density, to the concentration gradient of the chemical specie at that point. The steady state of the problem is obtained and a linear stability analysis of the coupled fields is made. The resulting eigenvalue-eigenfuction problem is presented, as well as the neutral stability curves for stationary disturbances, turning with the same angular velocity of the disk and for disturbances turning with angular velocity different from the disk one.

2. Governing Equations

The problem is governed by the continuity and the Navier-Stokes equations, coupled through the viscosity, to the transport equation of the relevant chemical specie. These equations, written in the frame attached to the surface of the rotating disk read:

$$\operatorname{div}\mathbf{v} = 0 \tag{1}$$

$$\frac{D\mathbf{v}}{Dt} = -2\boldsymbol{\Omega}\times\mathbf{v} - \boldsymbol{\Omega}\times(\boldsymbol{\Omega}\times\mathbf{r}) - \frac{1}{\rho}\,\mathbf{grad}\,p + \frac{1}{\rho}\operatorname{div}\tau \tag{2}$$

$$\frac{DC_T}{Dt} = \operatorname{div}(D\mathbf{grad}\,C_T) \tag{3}$$

where τ is the viscous stress tensor for a newtonian fluid with variable viscosity, C_T is the total concentration of the chemical specie and the factor D, multiplying the concentration gradient in Eq. (3) is the variable diffusion coefficient of the specie.

The evolution equations are written in non-dimensional form. Variables having units of length or its reciprocal (radial and axial coordinates, perturbation wavenumber along the radial direction) are made non-dimensional with the length used to measure the thikness of the boundary layer, $(\nu_\infty/\Omega)^{1/2}$, where ν_∞ is the bulk viscosity of the fluid. Velocity components are divided by the local imposed azimuthal velocity $r_e\Omega$, pressure is divided by the reference pressure $\rho(r_e\Omega)^2$, viscosity is divided by the bulk value, time and the eigenvalue of the linearized problem are made non-dimensional with the time required by a particle, turning with the azimuthal velocity $r_e\Omega$, to move a distance equal to the reference length, $(\nu_\infty/\Omega)^{1/2}$. Here, r_e is the dimensional coordinate along the radial direction where the stability analysis is carried. The non-dimensional concentration of the chemical specie is defined by:

$$C = \frac{C_T - C_\infty}{C_S - C_\infty} \tag{4}$$

We define also the Reynolds and the Schmidt numbers by the relations:

$$R = r_e^*\left(\frac{\Omega}{\nu_\infty}\right)^{1/2} \qquad \text{and} \qquad Sc = \frac{D_\infty}{\nu_\infty} \tag{5}$$

At this point, we assume that the viscosity depends on the concentration of the chemical specie, and, consequently, on the axial coordinate z. We also assume the Stokes-Einstein law, which postulates that the product of the diffusion coefficient by the viscosity is constant:

$$D\nu = D_\infty\,\nu_\infty \tag{6}$$

where D_∞ and ν_∞ are the bulk diffusion coefficient and the bulk viscosity, respectively. In adition, we assume that the viscosity varies with the concentration, according to:

$$\nu = \nu_\infty \exp(mC) \tag{7}$$

Using the bulk viscosity and diffusion coefficientes, ν_∞ and D_∞, to adimensionalize Eqs. (6) and (7) we obtain:

$$D\nu = 1 \qquad \text{and} \qquad \nu = \exp(mC) \tag{8}$$

Equations (1 – 3) take the following form, after introducing the adimensionalizing factors

$$\operatorname{div}\mathbf{v} = 0 \tag{9}$$

$$\frac{D\mathbf{v}}{Dt} = -2\,\mathbf{e}_z\times\mathbf{v} - \mathbf{e}_z\times\mathbf{grad}\,p + \frac{1}{R}\operatorname{div}\tau \tag{10}$$

$$\frac{DC_T}{Dt} = \frac{1}{R\,Sc}\operatorname{div}(D\,\mathbf{grad}\,C_T) \tag{11}$$

3. The Base State

3.1. Base state equations

The base state is the Von Kármán similarity solution for a fluid with the viscosity depending on the concentration field, which is assumed to vary along the axial coordinate only. In dimensional variables:

$$\begin{pmatrix} \bar{v}_r \\ \bar{v}_\theta \\ \bar{v}_z \\ p \\ \bar{C} \end{pmatrix} = \begin{pmatrix} r\,\Omega\,F(z) \\ r\,\Omega\,G(z) \\ (\nu_\infty\,\Omega)^{1/2}\,H(z) \\ \rho\nu_\infty\Omega P(z) \\ C_\infty + (C_S - C_\infty)C(z) \end{pmatrix} \tag{12}$$

Here, C_S and C_∞ are, respectively, the concentration of the chemical specie at the electrode surface and in the bulk. Boundary conditions for F, G, H and P are $F = G = H = P = 0$ at the disk surface ($z = 0$), $F = H' = P' = 0$ and $G' = -1$ in $z \longrightarrow \infty$. The non-dimensional concentration profile, C, varies from 1, $z = 0$, to 0, in $z \longrightarrow \infty$.

Eq. (12) is rewritten in nondimensional form:

$$\begin{pmatrix} \bar{v}_r \\ \bar{v}_\theta \\ \bar{v}_z \\ p \\ \bar{C} \end{pmatrix} = \begin{pmatrix} rF/R \\ rG/R \\ H/R \\ p/R^2 \\ C \end{pmatrix} \tag{13}$$

Introducing Eq. (13) in Eqs. (9 – 11), together with Eqs. (8), we obtain the ordinary nonlinear system for the axial profiles F, G, H, P and C:

$$2F + H' = 0 \tag{14}$$

$$F^2 - (G+1)^2 + HF' - \nu F'' - \nu' F' = 0 \tag{15}$$

$$2F(G+1) + HG' - \nu G'' - \nu' G' = 0 \tag{16}$$

$$P' + HH' - \nu H'' - 2\nu' H' = 0 \tag{17}$$

$$Sc\, HC' - \frac{C''}{\nu} + \frac{\nu'}{\nu^2} C' = 0 \tag{18}$$

where ν is given by Eq. (8) and

$$\nu' = m \exp(mC)\, C' \tag{19}$$

3.2. Evaluation of the Viscosity at the Electrode/Electrolyte Interface

Eqs. (14 – 18) are solved using the Newton method, in a uniform grid of points, with space derivatives represented by second order approximations. Solving these equations require specification of two parameters: the bulk Schmidt number ($Sc = 2000$) and the parameter m appearing in Eq. (7), which ultimately define de electrolyte viscosity at the interface with the electrode, where the non-dimensional concentration of the relevant chemical specie is equal to 1. Though both questions were adressed in a separate paper by the authors (Barcia 2005, submitted) we briefly review the key points of the subject for the sake of completness.

The bulk Schmidt number is easily estimated by noting that the viscosity of the 1 **M** $\mathbf{H_2SO_4}$ solution is $\nu_\infty = 1.0 \times 10^{-2} cm^2/s$ and the diffusion coefficient of the $\mathbf{Fe^{+2}}$ ion in the electrolyte is $D_\infty =$.

The limit current density at the interface is given by the relation:

$$i = nF \frac{1}{Sc} \frac{1}{\nu_0/\nu_\infty} \left(C^*_\infty - C^*_s\right) \sqrt{\nu_\infty \Omega}\, \left.\frac{dC}{dz}\right|_{z=0} \tag{20}$$

where i is expressed in A/cm^2, n is the valency number of the chemical specie ($n = 2$), $F = 96500\, C/mol$, is the Faraday constant, $C^*_s = 2.0 \times 10^{-3} mol/cm^3$ is the dimensional concentration of the specie at saturation conditions and $C^*_\infty = 0\, mol/cm^3$. The limit current density is obtained experimentaly as $i = 0.8810\, A/cm^2$ at $900\, rpm$. The remainning variables in Eq. (20), ν_0/ν_∞ and the nondimensional derivative of the concentration profile at the interface, $dC/dz|_{z=0}$, depend on the concentration profile, which is obtained by solving Eqs. (14 – 18). The profile is iteratively solved until the RHS of Eq. (20) converges to the experimental value of the limit current density. Convergence is attained for $\nu_0/\nu_\infty = 2.255$.

3.3. Base State Profiles

The high Schmidt number of the problem leads to a rather thin concentration boundary layer. The ratio between the thiknesses of the hydrodynamic (δ_h) and the concentration (δ_h) bondary layers is given, for the rotating disk flow problem, by (Levich, 1962):

$$\frac{\delta_h}{\delta_c} \approx 2\, Sc^{1/3} \tag{21}$$

The thin concentration boundary layer results in velocity profiles very close to the ones obtained for the constant viscosity case, outside the concentration boundary layer, which extends to $z \approx 0.25$. In particular, we obtain $H = -0.88559$ far from the disk for the variable viscosity flow considered, whereas $H = -0.88447$ for the constant viscosity case. The non-dimensional velocity, viscosity and concentration profiles, F, G, H, ν, the variable diffusion coefficient D and C, obtained for $\nu_0/\nu_\infty = 2.255$ and $Sc = 2000$ are shown in Fig. (1).

However, the derivatives of the velocity profiles are strongly affected by the concentration boundary layer, as shown in Fig. (2). Upon assuming a thickness of $\delta_h = 6$ for the hydrodynamic boundary layer we estimate a thickness of $\delta_c = 0.24$ for the concentration one, using Eq. (21). The profiles numerically obtained agree with this estimation.

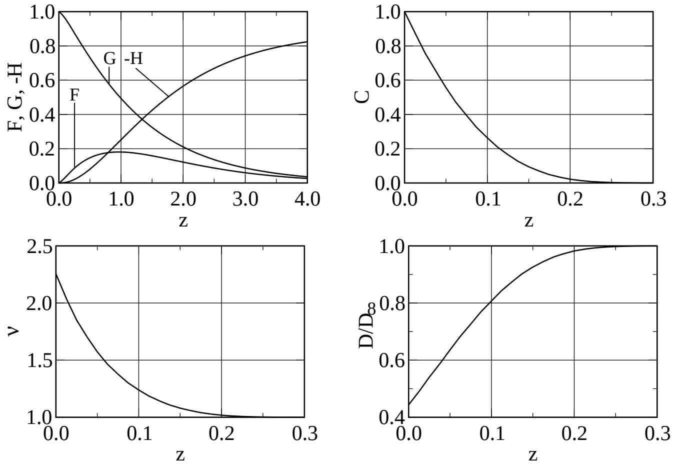

Figure 1: Dimensionless velocity, concentration and viscosity profiles for $\nu_0/\nu_\infty = 2.255$ and $Sc = 2000$.

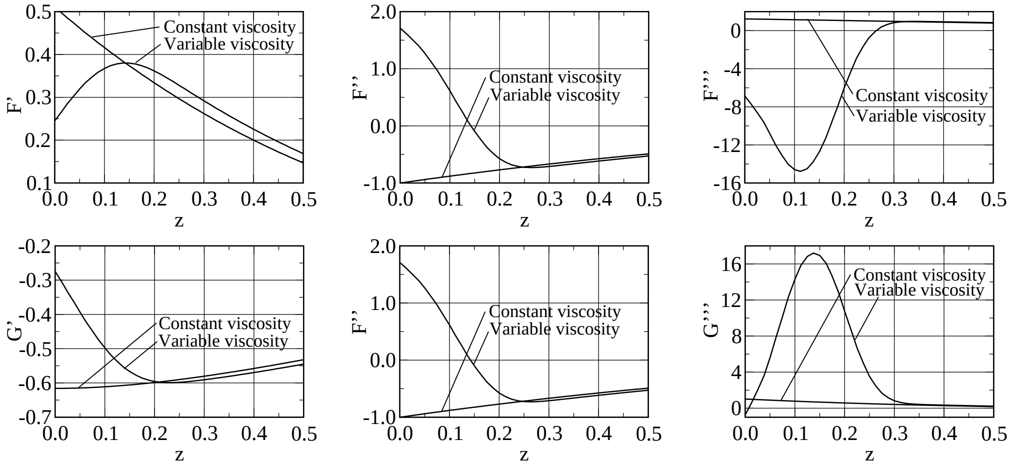

Figure 2: The first three derivatives of the non-dimensional velocity profiles, F and G, for the constant and variable viscosity cases.

4. Stability of the Base State

4.1. Stability equations

We turn now to the question of the stability of the base state with respect to small disturbances. The hydrodynamic and chemical fields are written as a summ of the base state plus a perturbation:

$$\left.\begin{array}{rclrclrcl} v_r &=& \bar{v}_r + \tilde{v}_r & v_\theta &=& \bar{v}_\theta + \tilde{v}_\theta & & & \\ v_z &=& \bar{v}_r + \tilde{v}_z & p &=& \bar{p} + \tilde{p} & C_T &=& \bar{C} + \tilde{C} \end{array}\right\} \qquad (22)$$

where the perturbation is given by, in dimensional form:

$$\begin{pmatrix} \tilde{v}_r \\ \tilde{v}_\theta \\ \tilde{v}_z \\ \tilde{p} \\ \tilde{C} \end{pmatrix} = \begin{pmatrix} r_e \Omega\, f \\ r_e \Omega\, g \\ r_e \Omega\, h \\ \rho \nu_\infty \Omega\, \pi \\ C_\infty + (C_s - C_\infty)\, c \end{pmatrix} \exp\left[i(\alpha r + \beta R \theta - \omega t)\right] + cc \qquad (23)$$

where ω is a complex number, with $\Re(\omega)$ and $\Im(\omega)$ being, respectively, the frequency and the rate of growth of the perturbation. The parameters α and β are the components of the perturbation wave-vector along the radial and azimuthal directions. For a given time, the phase of the perturbation is constant along branches of a logarithmic spiral, with the branches curved in the clockwise direction if β/α is positive and counter-clockwise, if negative. The structure turns counter-clockwise if ω/β is positive and clockwise, if negative. In non-dimensional form:

$$\begin{pmatrix} \tilde{v}_r \\ \tilde{v}_\theta \\ \tilde{v}_z \\ \tilde{p} \\ \tilde{c} \end{pmatrix} = \begin{pmatrix} f \\ g \\ h \\ \pi \\ c \end{pmatrix} \exp\left[i(\alpha r + \beta R\theta - \omega t)\right] + cc \tag{24}$$

The perturbation variables are introduced in Eqs. (9 – 11) and nonlinear terms are dropped. The parallel flow hypothesis is assumed, in order to confirm the assumption that perturbation variables are separable. To conclude, terms of order R^{-2} are dropped, leading to the following complex, non-symmetric, generalized eigenvalue-eigenfuction problem:

$$\begin{pmatrix} A_{11} & A_{12} & A_{13} \\ A_{21} & A_{22} & A_{23} \\ A_{31} & & A_{33} \end{pmatrix} \begin{pmatrix} h \\ \eta \\ c \end{pmatrix} = \omega R \begin{pmatrix} B_{11} & & \\ & B_{22} & \\ & & B_{33} \end{pmatrix} \begin{pmatrix} h \\ \eta \\ c \end{pmatrix} \tag{25}$$

where $\eta = \alpha g - \beta f$, missing elements in the matrices are zero and the operators A_{ij} and B_{ij} are given by:

$$\left.\begin{array}{lllllll} A_{11} & = & a_{114}D^4 + a_{113}D^3 + a_{112}D^2 + a_{111}D + a_{110} & & A_{12} & = & a_{121}D + a_{120} \\ A_{13} & = & a_{132}D^2 + a_{131}D + a_{130} & & A_{21} & = & a_{211}D + a_{210} \\ A_{22} & = & a_{222}D^2 + a_{221}D + a_{220} & & A_{23} & = & a_{231}D + a_{230} \\ A_{31} & = & a_{310} & & A_{33} & = & a_{332}D^2 + a_{331}D + a_{330} \\ & & & & & & \\ B_{11} & = & D^2 - \bar{\lambda}^2 \qquad B_{22} \; = \; 1 & & B_{33} & = & iSc \end{array}\right\}$$

where $D^n = d^n/dz^n$ and the coefficients a_{ijk} are given by:

$$a_{114} = i\nu \qquad a_{113} = i(2\nu' - H) \qquad a_{112} = i\nu'' - i\nu\left(\lambda^2 + \bar{\lambda}^2\right) + R\left(\alpha F + \beta G\right) - i\left(H' + F\right)$$

$$a_{111} = -i\nu'\left(\lambda^2 + \bar{\lambda}^2\right) + iH\bar{\lambda}^2 \qquad a_{110} = i\bar{\lambda}^2\left(\nu'' + \nu\lambda^2\right) - R\left(\alpha F + \beta G\right)\bar{\lambda}^2 - R\left(\bar{\alpha}F'' + \beta G''\right) + iH'\bar{\lambda}^2$$

$$a_{121} = 2\left(G + 1\right) \qquad a_{120} = 2G'$$

$$a_{132} = R\left(\bar{\alpha}F' + \beta G'\right)\gamma \qquad a_{131} = \left[2R\left(\bar{\alpha}F'' + \beta G''\right) + 6i\bar{\lambda}^2F\right]\gamma + 2R\left(\bar{\alpha}F' + \beta G'\right)\gamma'$$

$$a_{130} = \left(R\bar{\lambda}^2\left(\alpha F' + \beta G'\right) + R\left(\bar{\alpha}F''' + \beta G'''\right) + 4i\bar{\lambda}^2F'\right)\gamma + \left(2R\left(\bar{\alpha}F'' + \beta G''\right) + 6i\bar{\lambda}^2F\right)\gamma' + R\left(\bar{\alpha}F' + \beta G'\right)\gamma''$$

$$a_{211} = 2\left(G + 1\right) \qquad a_{210} = -iR\left(\alpha G' - \beta F'\right) \qquad a_{222} = i\nu \qquad a_{221} = i\left(\nu' - H\right)$$

$$a_{220} = -i\nu\lambda^2 + R\left(\alpha F + \beta G\right) - iF$$

$$a_{231} = iR\left(\alpha G' - \beta F'\right)\gamma \qquad a_{230} = iR\left(\left(\alpha G'' - \beta F''\right)\gamma + \left(\alpha G' - \beta F'\right)\gamma'\right)$$

$$a_{310} = R\,Sc\,C' \qquad a_{332} = -\frac{1}{\bar{\nu}} \qquad a_{331} = \frac{1}{\bar{\nu}}\left(\frac{\bar{\nu}'}{\bar{\nu}} + \frac{1}{\bar{\nu}}C'\gamma + Sc\,\bar{\nu}H\right)$$

$$a_{330} = iR\,Sc\left(\alpha F + \beta G\right) - \frac{1}{\bar{\nu}}\left(-\bar{\lambda}^2 + \frac{1}{\bar{\nu}}\left(\left(2\frac{\bar{\nu}'}{\bar{\nu}}\gamma - \gamma'\right)C' - \gamma C''\right)\right)$$

where $\gamma = d\nu/dC$. Boundary conditions of the problem require non-slip flow and vanishing axial component of the velocity at the electrode surface. These conditions are already fulfilled by the base-state, so the hydrodynamic field cannot be modified by the perturbation at the electrode surface. In consequence we must require $h = \eta = c = 0$ in $z = 0$. Moreover, we conclude from the continuity equation, that $h' = 0$ at the electrode surface. In $z \longrightarrow \infty$ we require that the perturbation vanishes ($h = \eta = c = 0$) and that $h' = 0$.

The eigenvalue-eigenfuction problem defined by Eq. (25) is solved numerically. Space derivatives are replaced by discrete second-order representations, transforming the original problem in an eigenvalue-eigenvector problem, which is solved through the inverse power method.

4.2. Results

The neutral stability curves for stationary disturbances and for disturbances turning with $\omega = 0.025$, obtained by solving the eigenvalue-eigenfunction problem are presented in Fig. 3. Figs. 3(a) and 3(b) show the neutral curves associated to the constant and the variable viscosity cases, in the $\alpha \times R$ and $\beta \times R$ plane, respectively. Fig. 3(c) shows the curves of the variable viscosity case, in the $\alpha \times \beta$ plane. This figure shows that the coupling of the mass concentration field to the hydrodynamic field through the variable viscosity affects the stability properties of the coupled fields, by strongly perturbing the neutral curve of the hydrodynamic modes and by introducing a new family of much more unstable modes, associated to the mass trasnport equation.

The critical Reynolds number of the hydrodynamic modes is reduced to approximately 50% of value for constant viscosity fluids. In addition, the unstable region is strongly enlarged and extends to modes with higher wavenumbers, than in the constant viscosity case. The neutral curve for constant viscosity fluids presents two minima, the second one occuring at $R \approx 440$ and being associated two a second unstable mode, which holds a profile along the axial direction which is different from the profile associated to the most unstable mode. This second mode is more affected by the variable viscosity field and becomes the most unstable hydrodynamic mode, in the variable viscosity case.

However, the new critical Reynolds number is now associated to the new unstable modes, which emerge from the modified flow dynamics, resulting from the coupling with the transport of the relevant chemical specie, through the concentration dependent viscosity. The new critical Reynolds number for stationary disturbances is $R = 52.3$, a number significantly smaller than 285.36, the critical value for constant viscosity fluids (Malik, 1986).

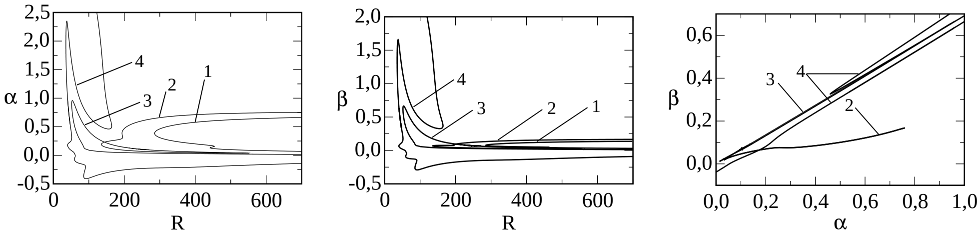

(*a*) (*b*) (*c*)

Figure 3: The neutral satbility curves of stationary perturbations ($\omega_r = 0.000$), in the $\alpha \times R$ (a), $\beta \times R$ (b) and $\alpha \times \beta$ (c) planes. Curves No. 1 refer to constant viscosity fluids; Curves No. 2 refer to the stability limit of the hydrodynamic mode associated to the variable viscosity case; Curves No. 3 refer to the stability limit of the chemical mode associated to the variable viscosity case. Curves No. 4 refer to perturbations turning with angular velocity $\omega = 0.025$. These last curves are preliminary.

5. Conclusions

In conclusion, we studied the effect of the coupling, of a mass concentration field, on the stability of the hydrodynamic field close to an iron rotating disk electrode. The mass concentration field is generated by the electro-dissolution of the electrode in a 1 **M** $\mathbf{H_2SO_4}$ solution and the coupling of the two fields occurs through the dependence of the viscosity, on the concentration of the chemical specie. The fluid viscosity at the electrode surface was evaluated using the experimental value of the current density. The critical Reynolds number of the hydrodynamic modes are reduced to approximately 50% of the value associated to constant viscosity flows and the unstable region is enlarged to much higher wavenumbers. In addition, a new class of unstable modes, associated to the transport dynamics of the relevant chemical specie emerges and the absolute minimum Reynolds number of the coupled fields locates in the new curve. The absolute minimum is $R = 52.3$, a number more than five times smaller than the critical Reynolds number for constant viscosity fluids, $R = 285.36$. The stability analysis was performed for stationary disturbances, turning with the angular viscosity of the electrode.

6. Acknowledgments

N. M. acknowledges financial support from CNPq (Brazil). The authors acknowledge the Center of Parallel Computing (NACAD/COPPE) of the Federal University of Rio de Janeiro, where the numerical calculations were performed.

7. References

Barcia, O. E., Mattos, O. R., and Tribollet, B., 1992, Anodic dissolution of iron in acid sulfate under mass transport control, “J. Eletrochem. Soc.”, Vol. 139, pp. 446–453.

Epelboin, I., Gabrielli, G., Keddam, M., Lestrach, J. C., and Takenouti, H., 1979, Passivation of Iron in Sulfuric acid Medium, “J. Eletrochem. Soc.”, Vol. 126, pp. 1632–1637.

Faller, A. J., 1991, Instability and Transition of the Disturbed Flow Over a Rotating Disk, “J. Fluid Mech.”, Vol. 230, pp. 245–269.

Ferreira, J. R. R. M., Barcia, O. E., and Tribollet, B., 1994, Iron dissolution under mass transport control: the effect of viscosity on the current oscillation, "Eletrochim. Acta", Vol. 39, pp. 933–938.

Geraldo, A. B., Barcia, O. E., Mattos, O. R., Huet, F., and Tribollet, B., 1998, New results concerning the oscillations observed for the system iron-sulphuric acid, "Electrochim. Acta", Vol. 44, pp. 455–465.

Levich, V. G., 1962, "Physicochemical Hydrodynamics", Prentice Hall, Englewood Cliffs, NJ.

Lingwood, R. J., 1995, Absolute instability of the boundary layer on a rotating disk, "J. Fluid Mech.", Vol. 299, pp. 17–33.

Malik, M. R., 1986, The Neutral Curve for Stationary Disturbances in Rotating-disk Flow, "J. Fluid Mech.", Vol. 164, pp. 275–287.

Pontes, J., Mangiavacchi, N., Barcia, O. E., Mattos, O. R., and Tribollet, B., 2005, Rotating Disk Flow Stability in electrochemical Cells: Effect of the Transport of a Chemical Specie, "Proceedings of the 18th International Congress of Mechanical Engineering", Ouro Preto, MG, Brasil. ABCM.

Pontes, J., Mangiavacchi, N., Conceição, A. R., Barcia, O. E., Mattos, O. E., and Tribollet, B., 2002, Instabilities in Electrochemical Systems with a Rotatinng Disk electrode, "J. of the Braz. Soc. of Mechanical Sciences", Vol. XXIV-3, pp. 139–148.

Pontes, J., Mangiavacchi, N., Conceição, A. R., Barcia, O. E., Mattos, O. E., and Tribollet, B., 2004, Rotating Disk Flow Stability in Electrochemical Cells: Effect of Viscosity Stratification, "Phys. Fluids", Vol. 16, No. 3, pp. 707–716.

Reed, H. L. and Saric, W. S., 1989, Stability of Three-Dimensional Boundary Layers, "Ann. Rev. Fluid Mech.", Vol. 21, pp. 235–84.

Russel, P. and Newman, J., 1986, Current oscillations observed within the limiting current plateau for iron in sulfuric acid, "J. Eletrochem. Soc.", Vol. 133, pp. 2093–2097.

Schäfer, P., Severin, J., and Herwin, H., 1995, The effect of heat transfer on the stability of laminar boundary layers, "Int. J. Heat Mass Transfer", Vol. 38-10, pp. 1855–1863.

Schlichting, H. and Gersten, K., 1999, "Boundary Layer Theory", Springer, Berlin.

Tribollet, B. and Newman, J., 1983, The modulated flow at a rotating disk electrode, "J. Eletrochem. Soc.", Vol. 130, pp. 2016–2026.

Turkyilmazoglu, M., Cole, J. W., and Gajjar, J. S. B., 1998, Absolute and Convective Instabilities in the Compressible Boundary Layer on a Rotating Disk, CLSCM Report CLSCM-1998-001, University of Manchester, Manchester.